N73-15818
NASA TM X-2685

NASA TECHNICAL MEMORANDUM

NASA TM X-2685

COLD-AIR AERODYNAMIC STUDY IN A TWO-DIMENSIONAL CASCADE OF A TURBINE STATOR BLADE WITH SUCTION-SURFACE FILM COOLING

by Douglas B. Brown and Ronald M. Helon

Lewis Research Center
Cleveland, Ohio 44135

NATIONAL AERONAUTICS AND SPACE ADMINISTRATION • WASHINGTON, D. C. • JANUARY 1973

1. Report No.	2. Government Accession No.	3. Recipient's Catalog No.
NASA TM X-2685		

4. Title and Subtitle	5. Report Date
COLD-AIR AERODYNAMIC STUDY IN A TWO-DIMENSIONAL CASCADE OF A TURBINE STATOR BLADE WITH SUCTION-SURFACE FILM COOLING	January 1973
	6. Performing Organization Code

7. Author(s)	8. Performing Organization Report No.
Douglas B. Brown and Ronald M. Helon	E-7106
	10. Work Unit No. 501-24

9. Performing Organization Name and Address	11. Contract or Grant No.
Lewis Research Center National Aeronautics and Space Administration Cleveland, Ohio 44135	

12. Sponsoring Agency Name and Address	13. Type of Report and Period Covered
National Aeronautics and Space Administration Washington, D.C. 20546	Technical Memorandum
	14. Sponsoring Agency Code

15. Supplementary Notes

16. Abstract

The effect on aerodynamic performance of a single row of spanwise-spaced coolant holes located at four positions chordwise along the suction surface was investigated. In addition, multiple-row data were obtained. The data are presented in terms of primary efficiency, coolant-to-primary-flow percentage, and coolant pressure ratio. Primary efficiencies of multirow blade configurations compare satisfactorily with that calculated from the single-row efficiency increments. At any given coolant flow percentage, the efficiency was about the same for all row locations. For a given coolant pressure, the efficiency varied by as much as 1 percent, depending on the row location.

17. Key Words (Suggested by Author(s))	18. Distribution Statement
Turbine cooling Cascade	Unclassified - unlimited

19. Security Classif. (of this report)	20. Security Classif. (of this page)	21. No. of Pages	22. Price*
Unclassified	Unclassified	30	$3.00

* For sale by the National Technical Information Service, Springfield, Virginia 22151

CONTENTS

COLD-AIR AERODYNAMIC STUDY IN A TWO-DIMENSIONAL CASCADE OF A TURBINE STATOR BLADE WITH SUCTION-SURFACE FILM COOLING

by Douglas B. Brown and Ronald M. Helon

Lewis Research Center

SUMMARY

A cold-air experimental investigation was conducted in a two-dimensional cascade to determine the aerodynamic performance of coolant ejection through four rows of holes on the suction surface of a turbine stator blade. The effect on aerodynamic performance of a single row of spanwise-spaced coolant holes located at four positions chordwise along the suction surface was investigated. In addition, multiple-row data were obtained. A range of primary-flow critical velocity ratios was covered with nominal set points at 0.48, 0.62, and 0.78. The effect of coolant discharge was investigated over a range of coolant-velocity-to-primary-air-velocity ratios from zero to 1.0.

The results of this investigation are, for the most part, presented in terms of primary efficiency, which relates the actual kinetic energy output of the mixed flow to the ideal kinetic energy of only the primary air.

Primary efficiencies of multirow blade configurations compare satisfactorily with that calculated from the single-row efficiency increments.

In general, the trend of primary efficiency is to increase with increasing coolant flow.

The effect on primary efficiency of coolant ejection at different locations on the blade surface was investigated. At any given coolant-to-primary-flow percentage, the efficiency was about the same for all coolant row locations. For a given coolant pressure, the primary efficiency varied by as much as 1 percent, depending on the row location.

The primary efficiency was affected by the presence of the coolant holes under a no-flow or low-coolant-flow condition. Surface roughness and primary inflow obscure the results under these conditions.

INTRODUCTION

To meet their performance requirements, many current and advanced gas turbine engines must operate at high turbine-inlet temperatures. These temperatures are high enough that the turbine blading must be cooled to avoid exceeding the stress and oxidation limitations of currently available materials. The general method for cooling the blading is to bleed air from the compressor, direct it through the turbine blading, and then discharge it from the blading into the main gas stream.

The means of discharging the coolant from the blading into the main gas stream vary. In reference 1, an analysis is presented which indicates that various means of coolant ejection affect turbine performance quite differently. An investigation is being conducted at the NASA Lewis Research Center to determine the effect on turbine-blade-row and stage performance of several means of coolant discharge that are typical of different cooled-blade designs. The results of some parts of this program which have been completed are reported in references 1 to 9. References 2 to 4 report the results of experimental and analytical investigations of the effects of turbine-stator-blade trailing-edge coolant ejection on turbine-stator and stage performance. References 5 to 8 report the results of experimental and analytical investigations of the effects of two types of stator-blade transpiration coolant discharge on turbine-stator and stage performance. Reference 9 summarizes the results of references 2 to 8. The main conclusions of these investigations were that coolant flow ejected from the trailing edge parallel to the main stream contributed significantly to the turbine-stage work output; whereas, coolant flow ejected normal to the blade surface through a porous skin covering the complete stator-blade surface contributed little or nothing to the turbine-stage work output.

This report describes a continuation of the effort to determine the effect of coolant discharge on the aerodynamic performance of turbine stator blades. A cold-air experimental investigation was conducted in a two-dimensional cascade with coolant discharge through four rows of spanwise-spaced holes located on the suction surface of a turbine stator blade. The effect on aerodynamic performance of a single row of coolant holes located at four positions chordwise along the suction surface was investigated. In addition, multiple-row data were obtained. A range of primary-flow critical velocity ratios was covered with nominal set points at 0.48, 0.62, and 0.78. The effect of coolant discharge was investigated over a range of coolant-velocity-to-primary-air-velocity ratios from zero to 1.0.

The data are presented in terms of primary and thermodynamic kinetic energy efficiencies as a function of the coolant-mass-flow-to-primary-mass-flow percentage and as a function of coolant total-pressure ratio. The coolant velocities can then be computed from this coolant pressure ratio. Experimentally determined coefficients of discharge for the coolant holes are included in the appendix.

BLADE DESCRIPTION

A detailed description of the blading used is given in reference 10. The subject blades have a constant cross section, corresponding to the mean-section profile of the reference stator blade. The span of the subject blade is 10.16 centimeters (4.0 in.) with a 5.74-centimeter (2.26-in.) chord. The blades are spaced on a 4.14-centimeter (1.63-in.) pitch. Figure 1 shows the velocity diagram, along with the blade geometry and spacing.

The locations of the rows of equi-spaced coolant holes are included in figure 1. Each row contains 83 holes of 0.076-centimeter (0.030-in.) diameter spaced 0.114 centimeter (0.045 in.) apart. Hereinafter the rows will be designated by their location, expressed as a percentage of the length along the suction surface from the leading edge to the trailing edge. The row locations, the hole angle, the length-diameter ratio of

a		β, deg	x/L_c, percent (a)	L/D
cm	in.			
0.572	0.225	35	20	4.2
1.923	.757	↓	40	4.0
3.307	1.302		60	3.8
4.630	1.823		80	3.8

[a] L_c = 7.12 cm (2.80 in.).

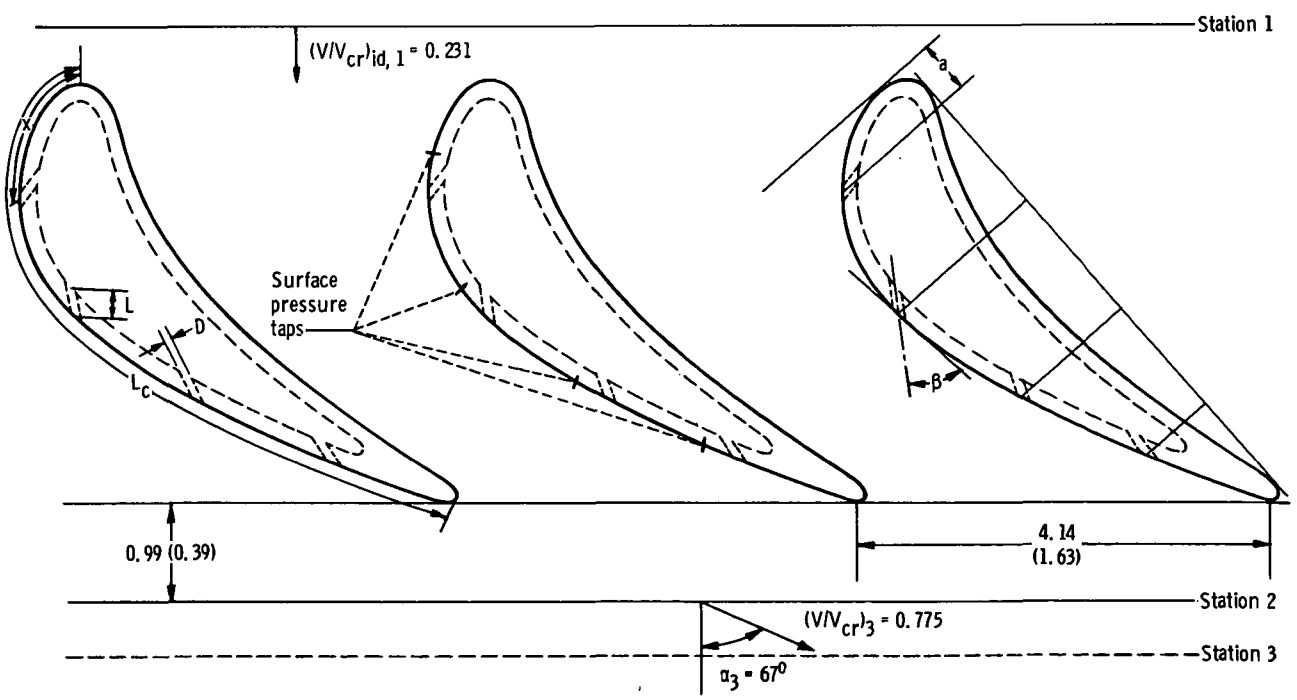

Figure 1. - Stator blade geometry. All dimensions are in cm (in.).

the holes, and the location of each row as a percentage of surface length are given in figure 1. Each hole is inclined at 35° with the local surface tangent.

Each row location will be referred to by indicating its percent location value. Multirow configurations will be designated by the number of rows in the configuration, which in turn specifies the particular rows present as follows:

Designation	Row locations present, percent
Two-row blade	20, 40
Three-row blade	20, 40, 60
Four-row blade	20, 40, 60, 80

Figure 2 shows the four-row blade tested. All configurations tested used this same blade with the appropriate row or rows filled and sealed with a talcum-dope solution and polished to form a smooth and continuous surface.

The pressure distribution measured over the surface of the blade is given in figure 3 for five critical velocity ratios. (This compares closely with the data reported in ref. 10.) This figure shows that the 20-percent location is in that region of the blade where the local surface pressure is higher than the exit static pressure. The other three row locations are in the region of the blade where local static pressures are lower than exit static pressure.

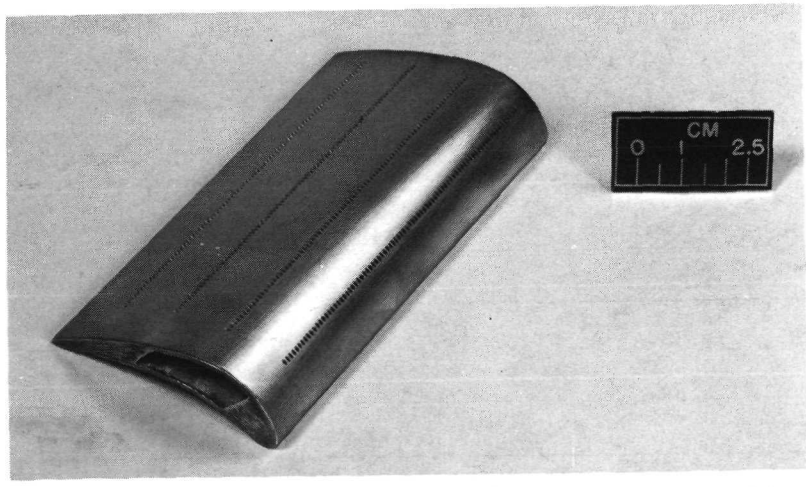

C-72-2178

Figure 2. - Stator blade.

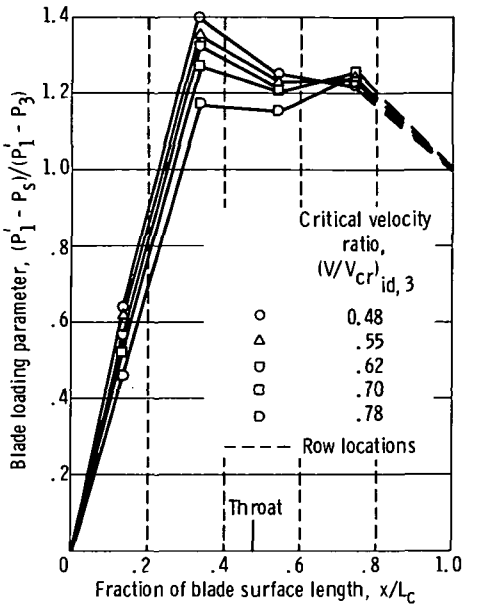

Figure 3. - Blade suction-surface pressures with all coolant holes sealed.

APPARATUS AND PROCEDURE

Cascade

The various coolant-row configurations were tested in the simple two-dimensional cascade shown in figure 4. The test blades occupied the middle three positions of the 12-blade cascade. Data were taken only with respect to the middle blade of the three blades so that similar conditions existed on either side of the test blade. Similarly, data were taken at the midspan position of the blading so that measurements would not be affected by end-wall effects.

In operation, room air was drawn through the inlet section and blading, through an exhaust control valve, and into the laboratory altitude exhaust system. The pressure ratio across the blade row was maintained by regulation of the exhaust control valve. The configurations were tested over a range of inlet-total- to exit-static-pressure ratios P_1'/P_3 with nominal set points at 1.15, 1.26, and 1.45. The corresponding values of exit ideal critical velocity ratio $\left(V/V_{cr}\right)_{id, 3}$ were 0.48, 0.62, and 0.78, respectively. One test series for one configuration then involved setting the exit static pressure at the selected value and recording data at zero coolant flow and then at a series of coolant flows all at the same exit static pressure.

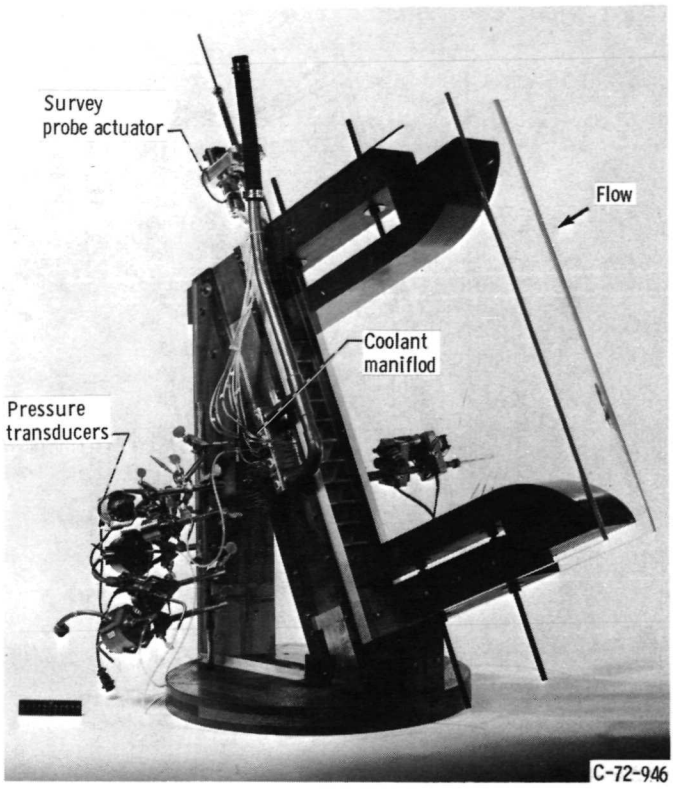

Figure 4. - Stator blade cascade.

Instrumentation

A calibrated multipurpose probe surveyed the flow conditions 2.54 centimeters (1.0 in.) in the direction of flow downstream of the blading. The probe continuously sensed total pressure, static pressure, and flow angle, with each parameter measured by a calibrated strain-gage pressure transducer. The type of probe used for the testing is shown in figure 5. Reference 11 gives a more detailed description of the probe.

Surface pressures were measured at four locations along the suction surface, as denoted by the hash marks in figure 1. These pressures were measured by mercury-filled manometers and recorded by photographing the manometer board.

Coolant total pressure was measured by assuming a reservoir condition inside the blade core. A movable probe was used to monitor the coolant total-pressure gradient inside the blade along the span.

Coolant flow was measured by various-sized calibrated sharp-edge orifices in an ASME-specified orifice run and computed as specified by ASME code.

Total flow was obtained by integration of probe survey data.

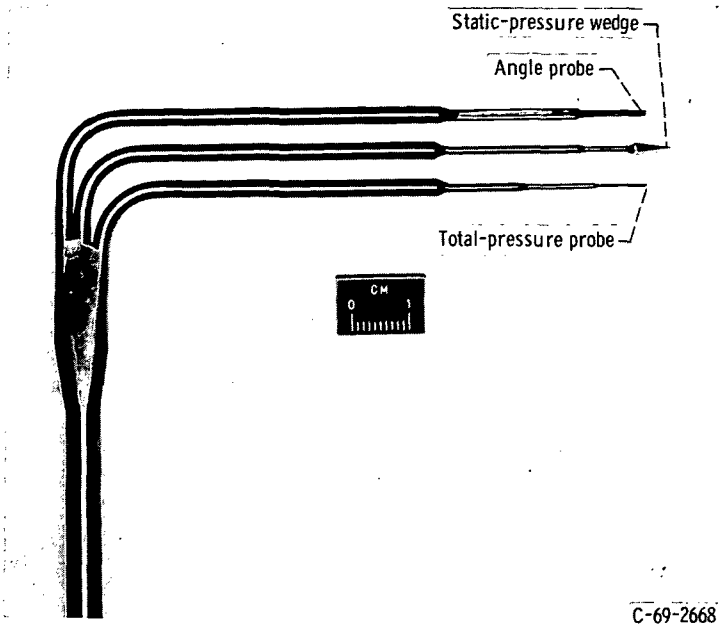

Figure 5. - Combination exit survey probe.

Data Reduction

Probe survey data were digitized and recorded on magnetic tape. The continuity equation, conservation of momentum, and energy relations were applied to a control volume to determine the aftermix downstream conditions. The control volume is 1 pitch wide, with its inlet plane coinciding with the survey plane and its downstream plane (designated station 3 in fig. 1) at a hypothetical location where flow conditions are assumed uniform.

The results are presented in terms of efficiencies based on this hypothetical constant-property location. Primary efficiency then is the ratio of actual kinetic energy of the combined flow to the ideal kinetic energy of the primary flow:

$$\eta_{p,3} = \frac{(m_c + m_p)V_3^2}{m_p V_{3,id,p}^2} \tag{1}$$

This primary efficiency can become greater than 1 since the ideal kinetic energy of only the primary flow is charged to the blade row.

The thermodynamic efficiency, however, charges the ideal energy of both the primary flow and the coolant flow to the blade row. This ideal energy is based on the re-

spective inlet total pressures and static downstream pressure, where coolant total pressure is the pressure in blade core:

$$\eta_{th,3} = \frac{(m_c + m_p)V_3^2}{m_p V_{3,id,p}^2 + m_c V_{3,id,c}^2} \tag{2}$$

RESULTS AND DISCUSSION

The results of the investigation are presented in four sections: Zero Coolant Flow Results, Single-Row Experimental Results, Multirow Experimental Results, and Combined Effects.

Zero Coolant Flow Results

For zero coolant flow, the definitions of primary and thermodynamic efficiencies given in equations (1) and (2) reduce to simply the square of the ratio of actual velocity to ideal velocity since no coolant flow is introduced.

The base efficiency of the blade was measured by filling and sealing all the coolant holes with the talcum-dope solution. Figure 6 shows the base efficiency measured for this "holes filled and sealed" configuration as a function of the critical velocity ratio $\left(V/V_{cr}\right)_{id,3}$. Efficiencies of 0.9745, 0.9745, and 0.9765 were measured for critical velocity ratios of 0.48, 0.62, and 0.78, respectively. In figure 6, the data of reference 12 are also shown to agree well.

Also shown in the figure are the efficiencies for the single-row configurations and for a configuration having all four rows of surface holes but with the blade core filled to prevent inflow. From these curves, it can be concluded that the physical presences of the holes affected the flow field to the extent that the primary efficiency was lowered by as much as 0.4 percent. The largest change by a single row was effected by the row at the 40-percent location, which was also the row location generally with the lowest local pressure and therefore the highest primary surface velocity, as indicated by figure 3. The lowest curve in figure 6 is that for four-row blade efficiencies with the core of the blade filled with a wax solution so that only the surface roughness of the blind holes affects the results. When the level of this last curve is compared to the curve for the 40-percent row location, it appears that the effect due to the presence of the holes is not additive. In other words, the presence of just the 40-percent location is enough to produce most of the effect.

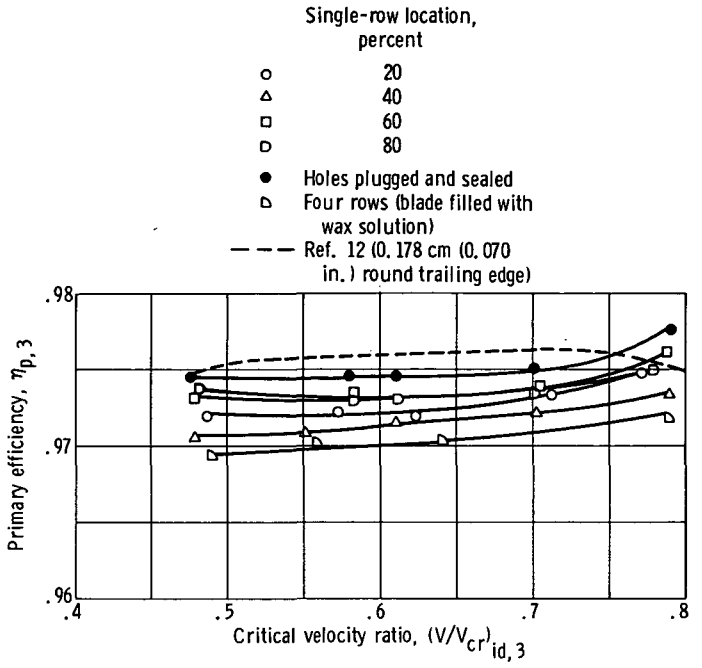

Figure 6. - Effect on primary efficiency of presence of coolant rows with zero coolant flow.

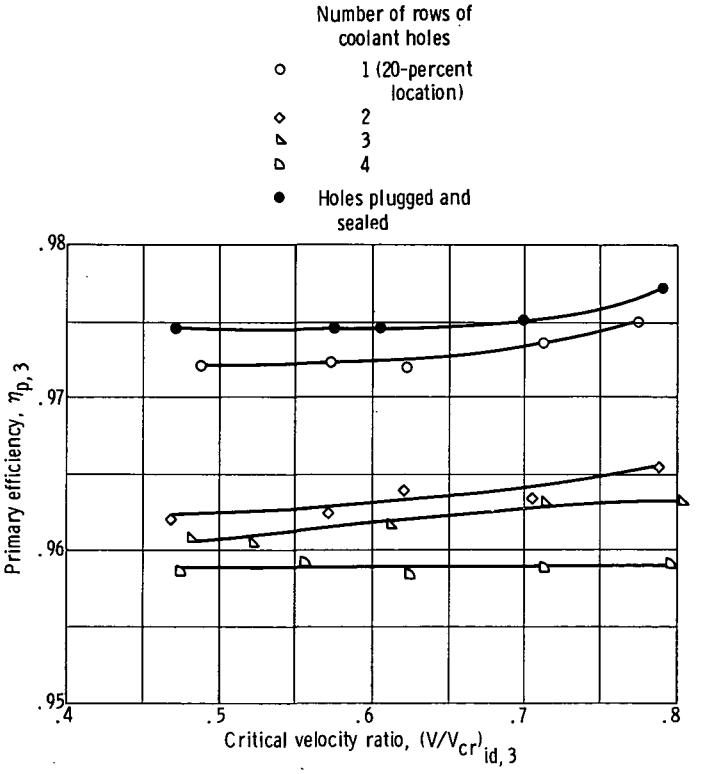

Figure 7. - Effect on primary efficiency of primary inflow in multirow configurations with zero coolant flow.

With the addition of more than one row, there is another factor that affects the efficiency. Figure 3 shows that at a given downstream critical velocity ratio $\left(V/V_{cr}\right)_{id,3}$ the static pressures vary over the surface of the blade. Thus, when there is more than one coolant row with holes open, primary flow can pass through the core between the row locations. Figure 7 shows this primary inflow effect on primary efficiency at various critical velocity ratios. As more than one row is added, the efficiency is reduced considerably more than the reduction due to the surface roughness effect shown in figure 6. It is therefore apparent that this decrease is caused by the primary air flowing through the core between coolant hole locations. This condition is of little practical significance, however, since coolant must flow out of all coolant holes to cool effectively.

Single-Row Experimental Results

A typical plot of the blade exit survey data is given as figure 8, where the loss in inlet total pressure is shown across 1 blade pitch in a plane corresponding to station 2 in figure 1. The effect of the addition of coolant flow can be seen by comparing these wake traces at varying amounts of coolant at one downstream critical velocity ratio $\left(V/V_{cr}\right)_{id,3}$. Figure 8 presents these data for three different ratios of coolant-mass-flow-to-primary-mass-flow percentage y. That is,

$$y = \frac{\dot{m}_c}{\dot{m}_p} \times 100$$

Figure 9 presents the results for the blade with a single row of holes located at four positions for three different critical velocity ratios. Primary efficiency is plotted against the coolant flow percentage. The general trend is for the efficiency first to drop relative to the sealed blade and then to increase, surpassing the base efficiency. Note that the primary efficiency does become greater than 1 since the ideal energy of only the primary flow is charged to the blade row. The continually increasing portion of the curve shows that, with increasing coolant flow, the total energy of the mixed flow is increased because of the addition of the energy of the coolant flow. The zero coolant effect due to the hole roughness described earlier can be recognized at $y = 0$. In general, the levels in figure 9 are the same for all row locations except the 40-percent location at low coolant flows, which is again the location of lowest surface pressure. The levels are also about the same for all critical velocity ratios. From figure 9 it can be seen that as much as 1.5-percent coolant flow is needed for the coolant hole

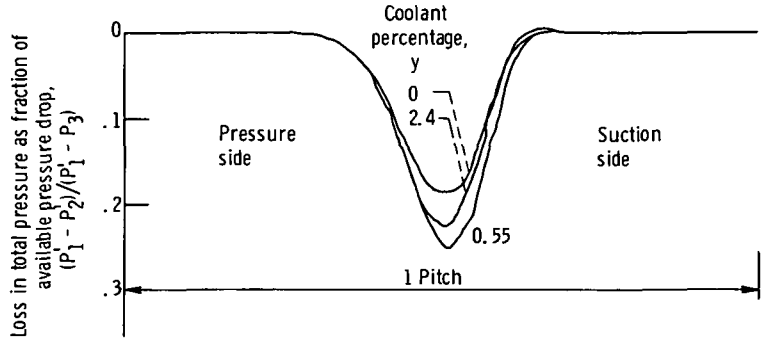

Figure 8. - Exit survey of loss in total pressure across 1 blade pitch. Row location, 20 percent; critical velocity ratio $(V/V_{cr})_{id,3}$, 0.78.

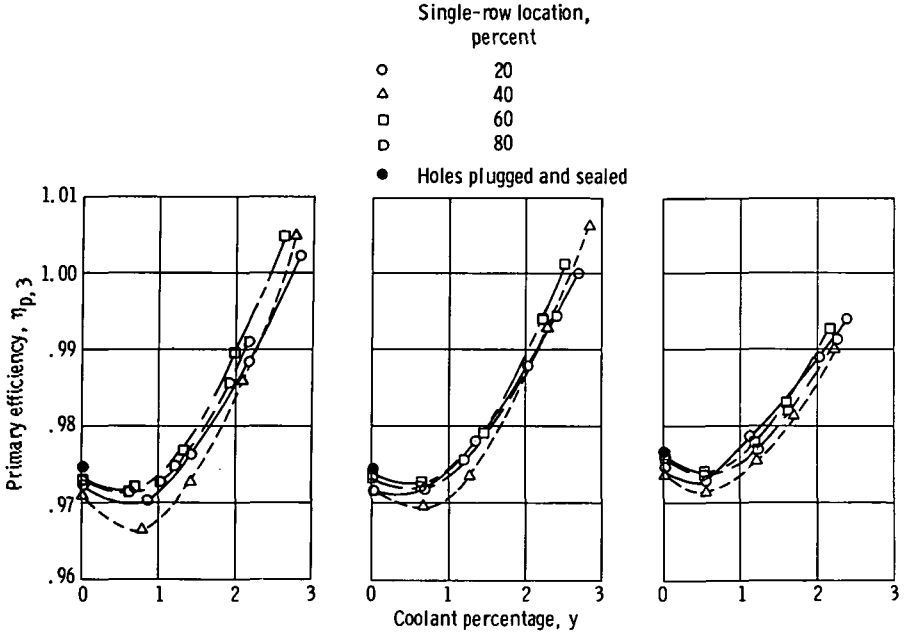

(a) Critical velocity ratio $(V/V_{cr})_{id,3}$, 0.48.

(b) Critical velocity ratio $(V/V_{cr})_{id,3}$, 0.62.

(c) Critical velocity ratio $(V/V_{cr})_{id,3}$, 0.78.

Figure 9. - Effect of coolant flow on primary efficiency for single-row configurations.

geometry tested before there will be an increase in the primary efficiency relative to that of the uncooled blade.

Figure 10 shows the same single-row data at the high critical velocity ratio with the thermodynamic efficiency also plotted. The trend for the thermodynamic efficiency is to decrease with increasing coolant flow. When comparing thermodynamic efficiencies for different row locations, it should be noted that not only might the actual kinetic energy be different for a given coolant percentage, but also the ideal kinetic energies

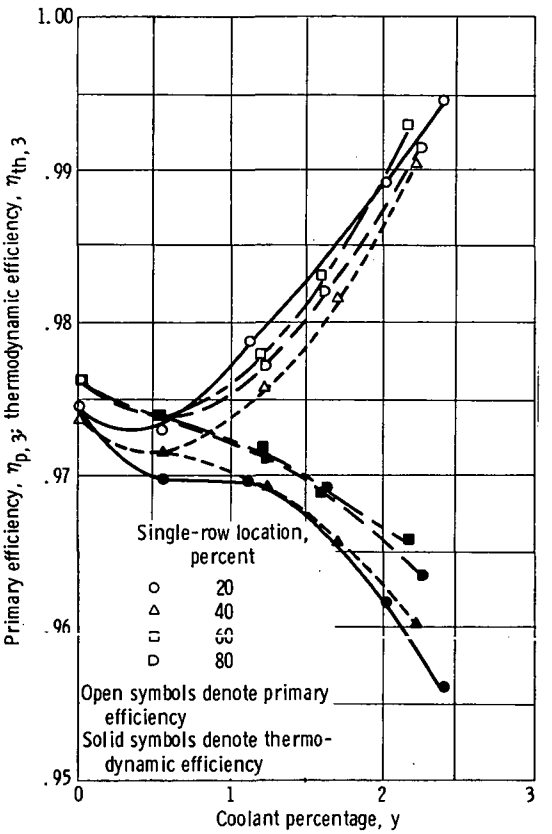

Figure 10. - Effect of coolant flow on efficiency for single-row configurations at critical velocity ratio $(V/V_{cr})_{id,3}$ of 0.78.

may be different since the coolant total pressures are not necessarily the same for corresponding coolant percentages.

Multirow Experimental Results

Figure 11 is similar to figure 8 in that it is a typical plot of the blade exit survey data. This figure is a representative sample of the data taken for the four-row blade

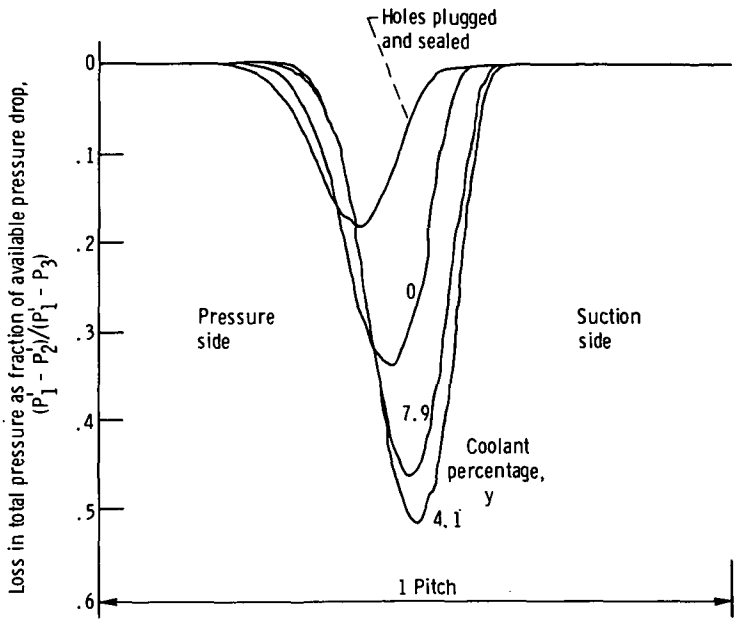

Figure 11. - Exit survey of loss in total pressure across 1 blade pitch. Four-row configuration; critical velocity ratio $(V/V_{cr})_{id,3}$, 0.78.

at a critical velocity ratio of 0.78. Note the difference in the wake region for the sealed-hole configuration and for the holes-open configuration with no coolant flow. This difference is caused by the effect of primary inflow and surface roughness, as discussed in the section Zero Coolant Flow Results.

Figure 12 presents primary efficiency against coolant percentage for the three different multirow configurations: two row, three row, and four row. Also, for reference, the single-row data for the 20-percent location are reproduced. The trend for each configuration is basically the same as for the single-row data: first, a lower level of efficiency relative to the sealed base blade, and then an increase in the efficiency, surpassing the base blade efficiency. For the hole geometry tested, 4.2- to 4.9-percent coolant flow (depending on the critical velocity ratio) is needed before the primary efficiency exceeds the efficiency of the base, or uncooled, blade.

As discussed in the section on zero flow results, at zero or low coolant flows there may be primary flow between the coolant rows through the blade core. Ticks on the curves of multirow data show where this inflow condition stops.

Figure 12 shows the importance of coolant velocity on efficiency. The single-row data have a higher level of efficiency than the multirow data because, at one coolant percentage, the coolant velocity is more for the single-row configuration than the multirow since the total coolant hole flow area is the smallest for the single row.

The thermodynamic efficiency at a critical velocity ratio of 0.78 is shown for the multirow data in figure 13. Thermodynamic efficiency for multirow configurations tends,

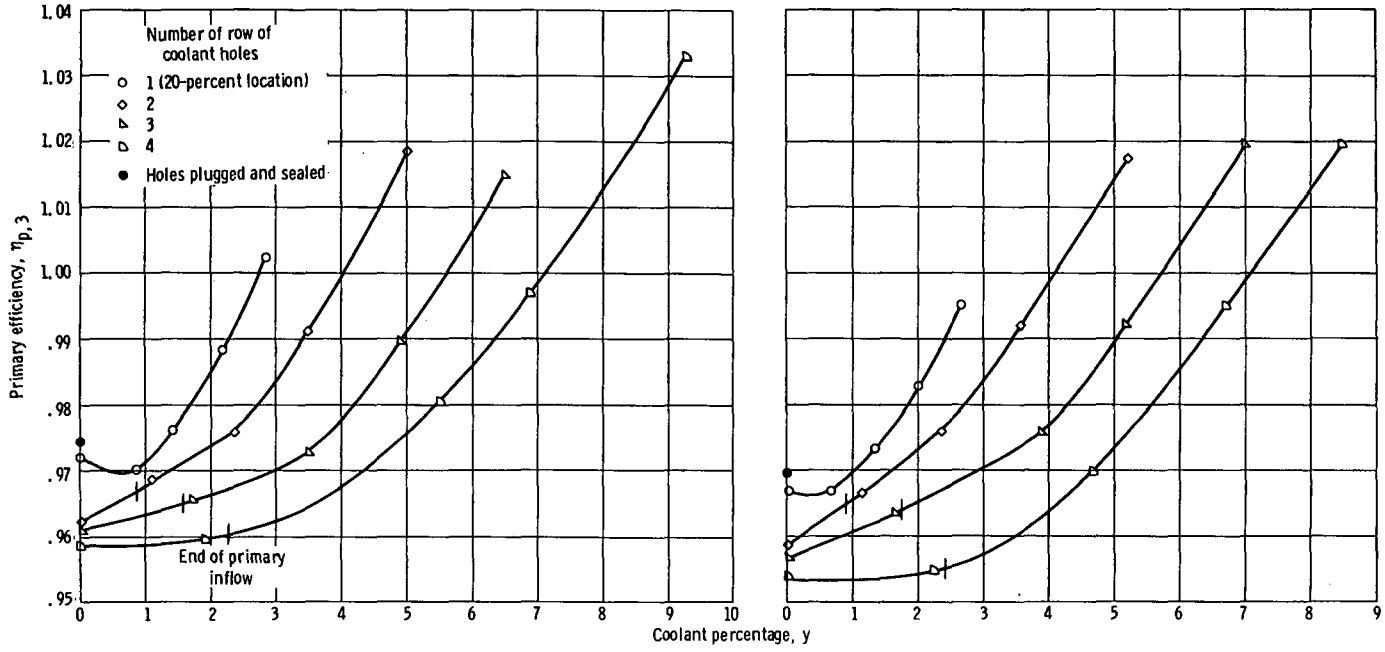

(a) Critical velocity ratio $(V/V_{cr})_{id,3'}$ 0.48.

(b) Critical velocity ratio $(V/V_{cr})_{id,3'}$ 0.62.

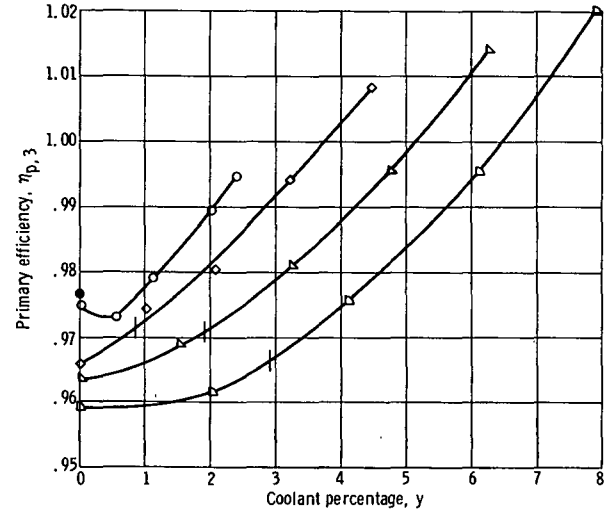

(c) Critical velocity ratio $(V/V_{cr})_{id,3'}$ 0.78.

Figure 12. - Effect of coolant flow on primary efficiency for multirow configurations.

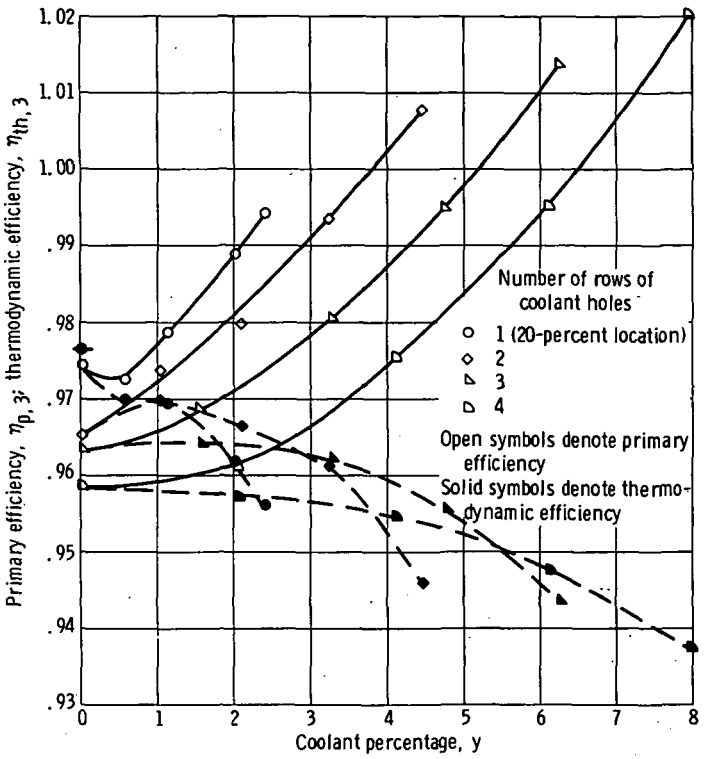

Figure 13. - Effect of coolant flow on efficiency for multirow configurations at critical velocity ratio $(V/V_{cr})_{id,3}$ of 0.78.

as noted for the single-row data, to decrease with increasing coolant flow.

Combined Effects

Single-row data and multirow data are shown in figure 14. Coolant flow percentage is shown as a function of coolant pressure drop to primary pressure drop for the three critical velocity ratios. For one critical velocity ratio, P'_1 and P_3 are fixed so that the pressure drop ratio is directly proportional to P'_c. From this figure the amount of coolant percentage flowing through each row can be predicted. The amount of coolant percentage for the multirow configurations at which all rows have outward coolant flow can be seen in figure 14 at the pressure ratio where the 20-percent row just begins flowing. These points are marked in figure 12. Since the cascade has a fixed geometry, all flow conditions cannot be held constant for each configuration. Any variation in primary flow, however, for each configuration at a given coolant flow is believed to be of second order.

As more coolant flow passes through the blade core, the assumption of the core acting like a reservoir becomes less valid. Thus, for the multirow configurations at high

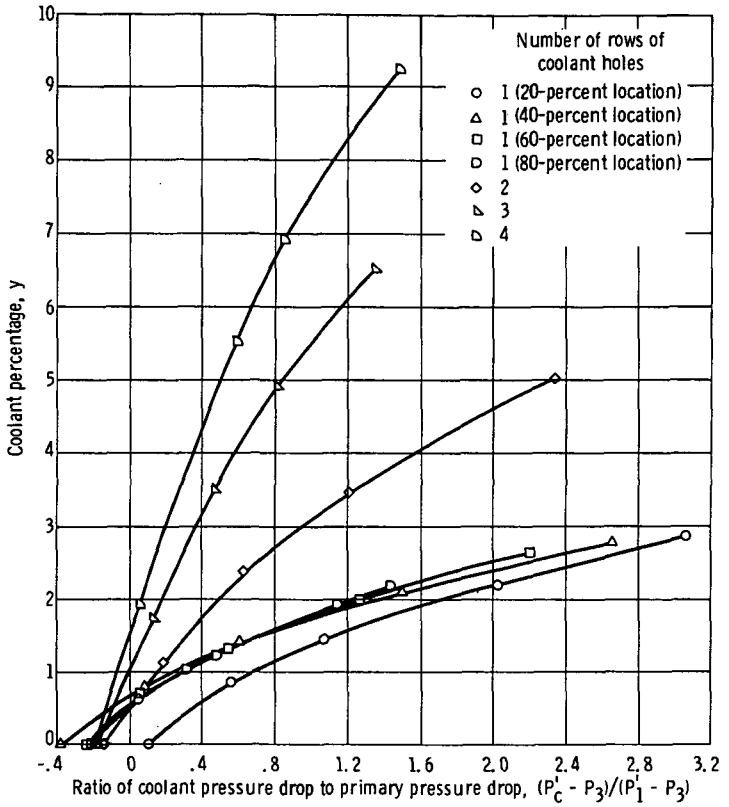

(a) Critical velocity ratio $(V/V_{cr})_{id,3'}$ 0.48.

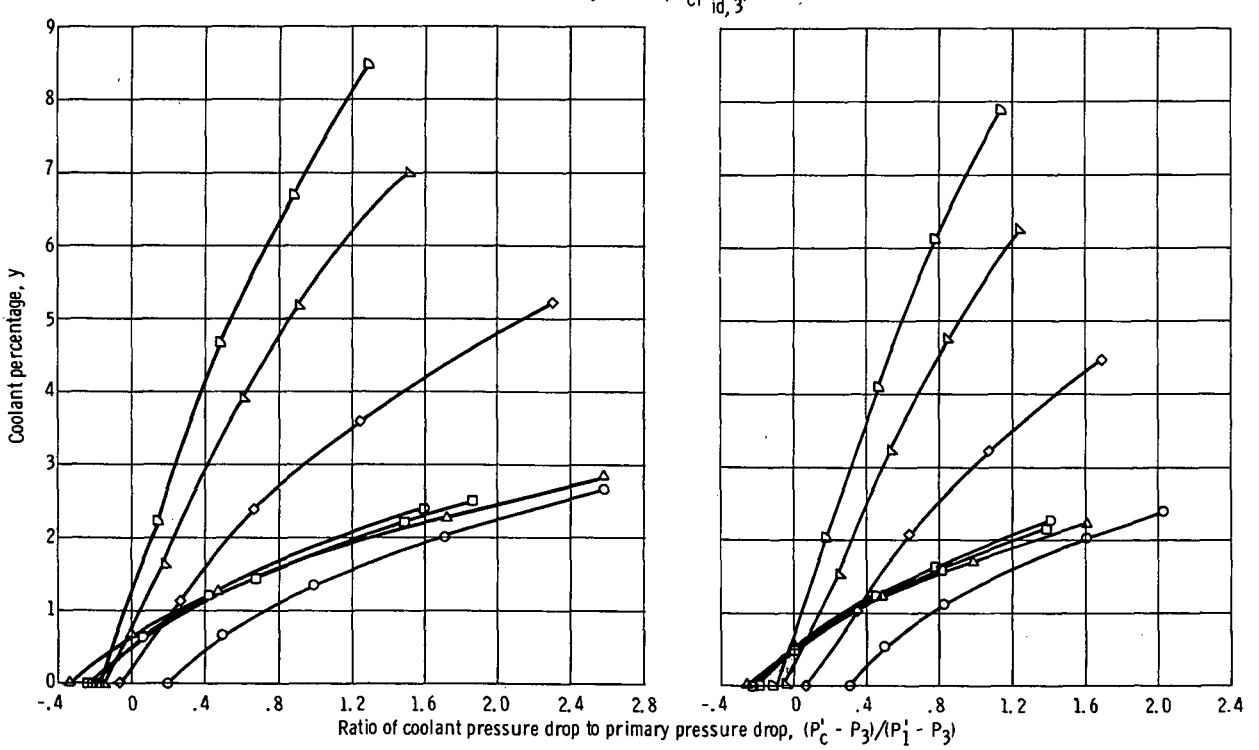

(b) Critical velocity ratio $(V/V_{cr})_{id,3'}$ 0.62.

(c) Critical velocity ratio $(V/V_{cr})_{id,3'}$ 0.78.

Figure 14. - Coolant flow distribution in multirow configuration.

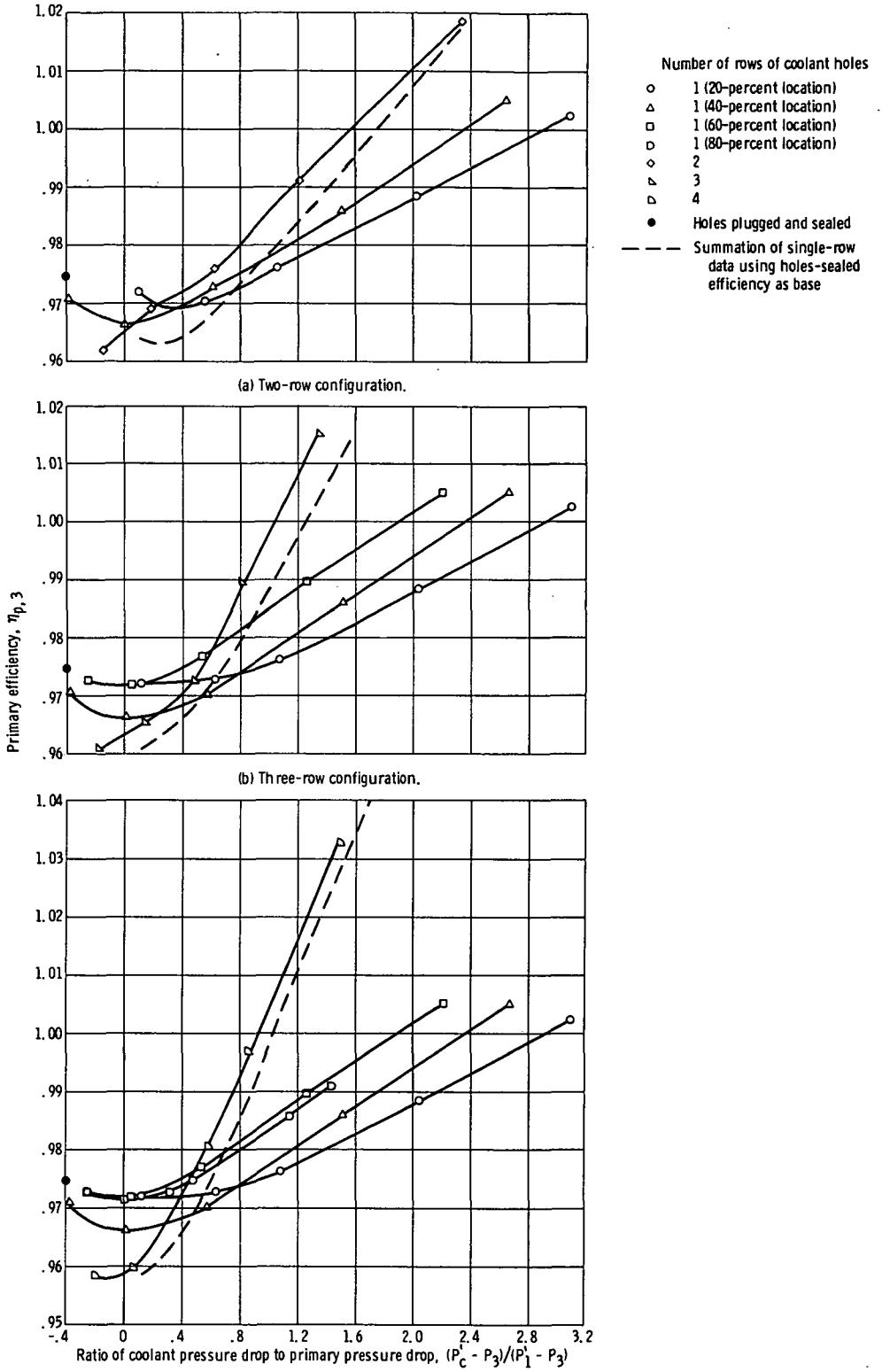

(a) Two-row configuration.

(b) Three-row configuration.

(c) Four-row configuration.

Figure 15. - Contribution of single-row blade primary efficiencies to multirow-blade-configuration primary efficiencies for critical velocity ratio $(V/V_{cr})_{id,3}$ of 0.48.

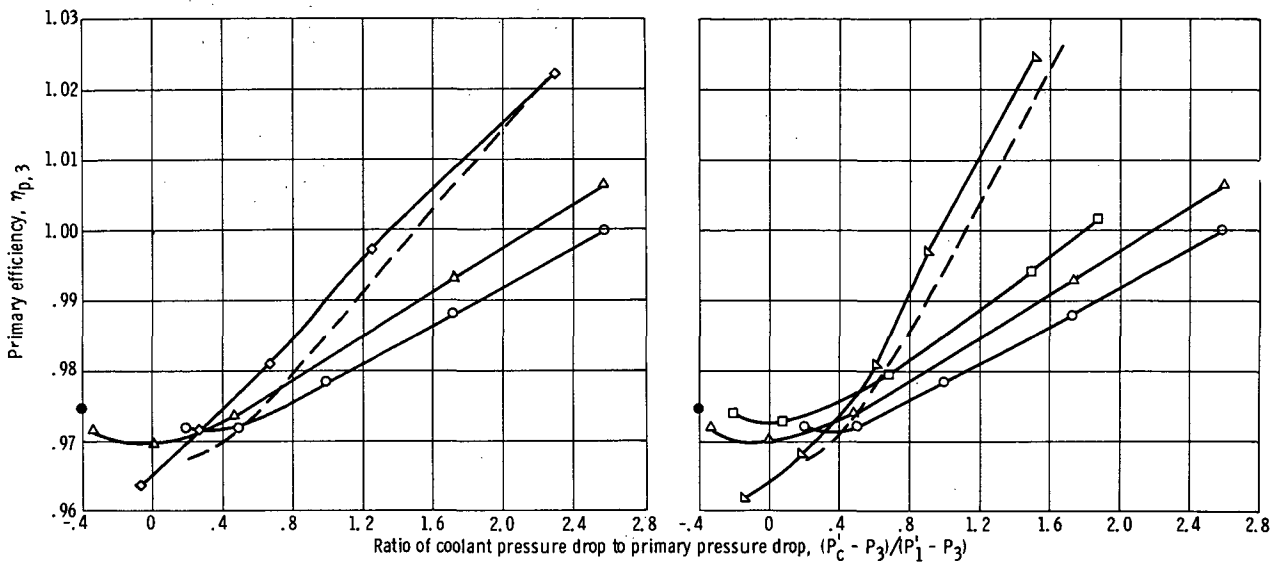

(a) Two-row configuration.

(b) Three-row configuration.

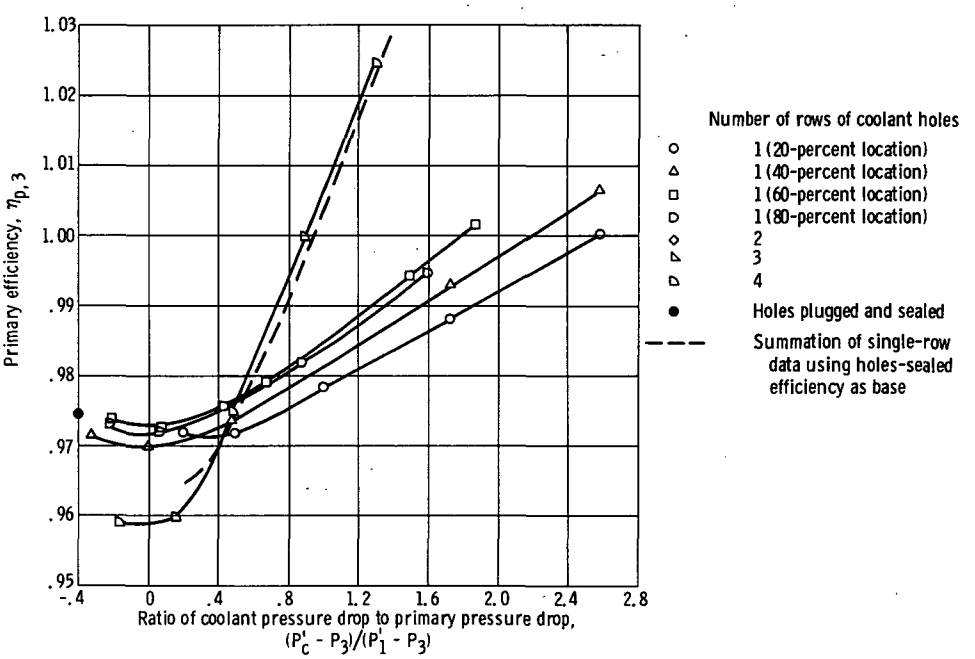

(c) Four-row configuration.

Figure 16. - Contributions of single-row blade primary efficiencies to multirow-blade-configuration primary efficiencies for critical velocity ratio $(V/V_{cr})_{id,3}$ of 0.62.

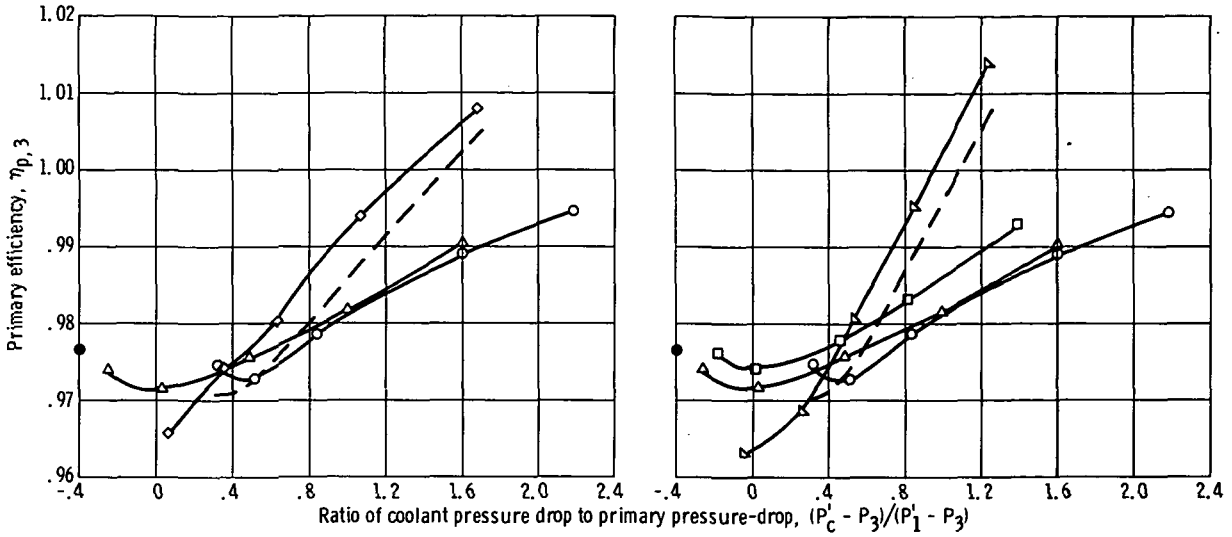

(a) Two-row configuration.

(b) Three-row configuration.

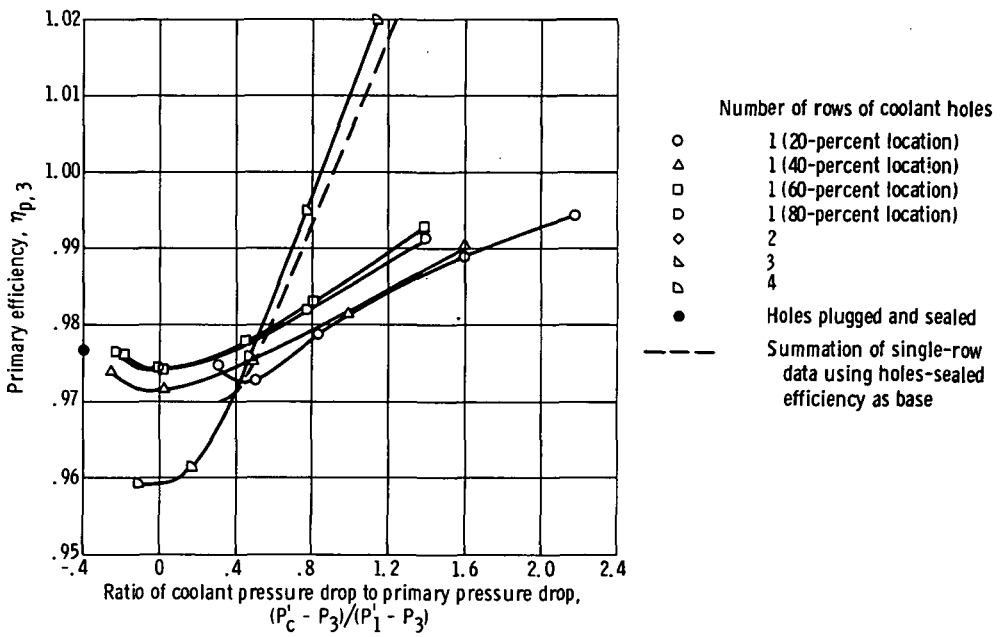

(c) Four-row configuration.

Figure 17. - Contribution of single-row blade primary efficiencies to the multirow-blade-configuration primary efficiencies for critical velocity ratio $(V/V_{cr})_{id,3}$ of 0.78.

coolant flows, the coolant pressure measured may not be a true total pressure.

Of interest is the contribution that each row makes to the change in primary efficiency relative to the base efficiency. The parameter common to all row locations in a multirow blade is the blade core total pressure P'_c since the inlets to all locations are fed by the same reservoir. A plot of efficiency against the ratio of coolant pressure drop to primary pressure drop for all configurations then will show the effect of each row on the efficiency of a multirow configuration. Figures 15, 16, and 17 show these results for the critical velocity ratios of 0.48, 0.62, and 0.78, respectively. Parts (a), (b), and (c) of each figure give the data for the two-row, three-row, and four-row configurations, respectively, and the single-row data applicable to each configuration. For each point on the multirow data curve, the change in efficiency relative to the base efficiency will be reflected by the addition of the change in efficiency of the single-row configurations at the same pressure ratio. This summation of the single-row-data change in efficiencies for the multirow configuration in question is presented in figures 15 to 17 as a dotted line. There are second-order effects that make this analysis not precise. In order to add the efficiencies, the ideal output in the denominator of equation (1) must be the same for a constant value of coolant pressure ratio. In general, this will not be the case since the cascade has a fixed geometry that cannot accommodate changes in primary flow. However, as seen from the figure, this procedure gives a reasonable approximation to the multirow performance except at very low coolant percentages. This approximation then could be used to estimate multirow performance of blades that have not been tested, for example, a 20- or 60-percent row location configuration.

Although it was stated earlier that all row locations had about the same primary efficiency at one coolant flow percentage, figures 15 to 17 show that at one coolant total pressure and one critical velocity ratio, the efficiencies of each row location may vary by 1 percent. This variation is caused by the different amounts of coolant flow percentages at each row location for one coolant pressure as a result of the varying surface pressures along the blade. These figures show the rank of the row locations in the order of increasing primary efficiency to be the 20-, 40-, 80-, and 60-percent locations for all primary critical velocity ratios.

SUMMARY OF RESULTS

A cold-air experimental investigation was conducted in a two-dimensional cascade to determine the aerodynamic performance of coolant ejection through four rows of holes on the suction surface of a turbine stator blade. The effect on aerodynamic performance of a single row of spanwise-spaced coolant holes located at four different positions

chordwise along the suction surface was investigated. In addition, multiple-row data were obtained.

The results of this investigation are, for the most part, presented in terms of primary air efficiency, which relates the actual kinetic energy of the combined flow to the ideal kinetic energy of only the primary air. A limited amount of results are shown in terms of thermodynamic efficiency. The findings were as follows:

1. There is a satisfactory comparison of primary efficiencies of multirow blade configurations with that calculated from the single-row efficiency increments.

2. In general, the trend of primary efficiency is to increase with increasing coolant flow since the ideal energy of the coolant is not charged to the blade row and the added coolant energy increases the actual blade-row output. The trend for thermodynamic efficiency is to decrease with increasing coolant flow.

3. In general, for the single-row configurations, the efficiencies are approximately the same at all surface locations for the same coolant flow fraction.

4. For a constant coolant total pressure, primary efficiency increases for different blade suction-surface locations in the following order: 20-, 40-, 80-, and 60-percent locations. The difference in efficiencies is as much as 1 percent.

Lewis Research Center,
National Aeronautics and Space Administration,
Cleveland, Ohio, October 4, 1972,
501-24.

APPENDIX A

SYMBOLS

A	area, m^2; ft^2
a	distance along chord from leading edge, cm; in.
C_D	discharge coefficient, ratio of actual flow to ideal flow
D	diameter of coolant hole, cm; in.
g	conversion constant, 1; 32.17 (lbm-ft)/(lbf-sec^2)
L	coolant hole length, cm; in.
L_c	suction-surface length on a radial plane from leading-edge stagnation point to trailing-edge stagnation point (see fig. 1), cm; in.
m	mass flow rate, kg/sec; lbm/sec
P	absolute pressure, N/m^2; lbf/ft^2
R	gas constant, 287 J/kg-K; 53.34 ft-lb/lb-^oR
T	temperature, K; ^oR
V	absolute velocity; m/sec; ft/sec
x	local position along suction surface from leading edge (see fig. 1), cm; in.
y	coolant percentage, $(m_c/m_p) \times 100$
α	flow angle, from axial direction, deg
β	angle between coolant-hole centerline and local blade-surface tangent, deg
γ	ratio of specific heats
δ	ratio of inlet pressure to U.S. standard sea-level pressure
η_p	stator primary-air efficiency, ratio of stator kinetic energy to ideal kinetic energy of primary flow (eq. (1))
η_{th}	stator thermodynamic efficiency, ratio of stator kinetic energy to ideal kinetic energy of both primary and coolant flows (eq. (2))
ρ	density, kg/cm^3; lbm/ft^3
θ_{cr}	squared ratio of critical velocity to critical velocity of U.S. standard sea-level air

Subscripts:

act	actual quantity

c coolant (secondary) flow

cr conditions at Mach 1

id ideal quantity corresponding to isentropic process

p primary flow

s blade-surface location

0 conditions with no primary flow

1 station at blade inlet

2 blade-exit survey station

3 station at blade exit where flow conditions are assumed uniform

Superscript:

' total-state conditions

APPENDIX B

SINGLE-HOLE DISCHARGE COEFFICIENTS

Experimentally determined discharge coefficients were calculated from the reported data for each of the four coolant row locations. The discharge coefficient is defined as the ratio of actual flow rate to ideal flow rate:

$$C_D = \frac{m_{act}}{m_{id}}$$

where m_{act} is a measured quantity and m_{id} is calculated from

$$m_{id} = \rho_{id} V_{id} A_{id}$$

$$\rho_{id,c} = \frac{P_s}{RT'_c}\left(\frac{P'_c}{P_s}\right)^{(\gamma-1)/\gamma}$$

$$V_{id,c} = \left\{\left(\frac{2\gamma}{\gamma - 1}\right) gRT'_c\left[1 - \left(\frac{P_s}{P'_c}\right)^{(\gamma-1)/\gamma}\right]\right\}^{1/2}$$

A_{id} = Physical hole area

A similar method to the one used by Lewis' Turbine Cooling Branch to correlate coefficient-of-discharge data was used here in order to take into account the effect on C_D of primary free-stream velocity at the exit of the coolant hole. The method suggests plotting a coefficient-of-discharge ratio against the ratio of ideal coolant momentum to ideal free-stream momentum $(\rho v^2)_{c,id}/(\rho v^2)_{p,id}$, where the primary flow parameters are given by

$$\rho_{p,id} = \frac{P_s}{RT'_p}\left(\frac{P'_1}{P_s}\right)^{(\gamma-1)/\gamma}$$

$$V_{id,p} = \left\{ \left(\frac{2\gamma}{\gamma - 1} \right) gRT'_p \left[1 - \left(\frac{P_s}{P'_1} \right)^{(\gamma-1)/\gamma} \right] \right\}^{1/2}$$

The coefficient-of-discharge ratio is the ratio of the coefficient of discharge C_D to the coefficient of discharge at zero free-stream flow $C_{D,0}$ evaluated at the same equivalent coolant flow rate.

Figure 18 shows the results for the 20-, 40-, 60-, and 80-percent locations, respectively, for the three reported primary critical velocity ratios $\left(V/V_{cr}\right)_{id,p,3}$. The results in figure 19 show a good correlation for all the data except the lower critical velocity ratio for the 40- and 60-percent locations. Figure 19 gives the coefficient of discharge against coolant ideal equivalent flow for the condition of no primary flow.

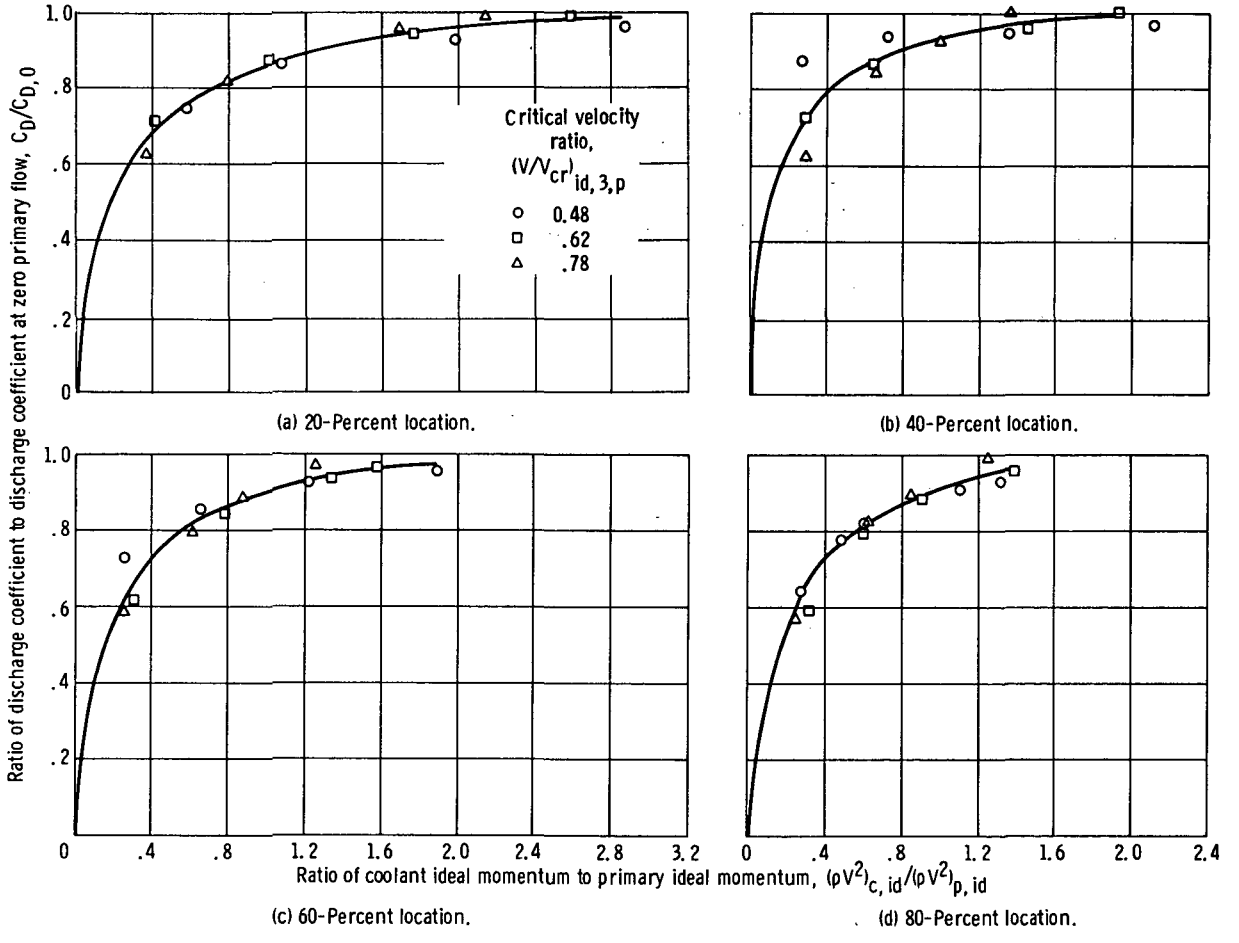

Figure 18. - Ratio of discharge coefficients for single-row configurations as function of momentum ratio. Angle between coolant-hole centerline and local blade-surface tangent, β, 35^0.

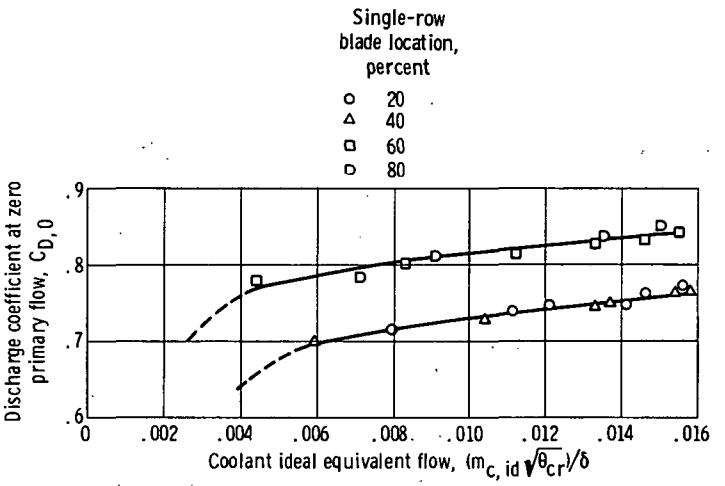

Figure 19. - Discharge coefficient for all row locations as function of equivalent flow for zero primary flow. Angle between coolant-hole centerline and local blade-surface tangent, β, 35^0.

REFERENCES

1. Whitney, Warren J.: Analytical Investigation of the Effect of Cooling Air on Two-Stage Turbine Performance. NASA TM X-1728, 1969.

2. Whitney, Warren J.; Szanca, Edward M.; and Behning, Frank P.: Cold-Air Investigation of a Turbine with Stator-Blade Trailing-Edge Coolant Ejection. I - Overall Stator Performance. NASA TM X-1901, 1969.

3. Prust, Herman W., Jr.; Behning, Frank P.; and Bider, Bernard: Cold-Air Investigation of a Turbine with Stator-Blade Trailing-Edge Coolant Ejection. II - Detailed Stator Performance. NASA TM X-1963, 1970.

4. Szanca, Edward M.; Schum, Harold J.; and Prust, Herman W., Jr.: Cold-Air Investigation of a Turbine with Stator-Blade Trailing-Edge Coolant Ejection. III - Overall Stage Performance. NASA TM X-1974, 1970.

5. Prust, Herman W., Jr.; Schum, Harold J.; and Szanca, Edward M.: Cold-Air Investigation of a Turbine with Transpiration-Cooled Stator Blades. I - Performance of Stator with Discrete Hole Blading. NASA TM X-2094, 1970.

6. Szanca, Edward M.; Schum, Harold J.; and Behning, Frank P.: Cold-Air Investigation of a Turbine with Transpiration-Cooled Stator Blades. II - Stage Performance with Discrete Hole Stator Blades. NASA TM X-2133, 1970.

7. Behning, Frank P.; Prust, Herman W., Jr.; and Moffitt, Thomas P.: Cold-Air Investigation of a Turbine with Transpiration-Cooled Stator Blades. III - Performance of Stator with Wire-Mesh Shell Blading. NASA TM X-2166, 1971.

8. Behning, Frank P.; Schum, Harold J.; and Szanca, Edward M.: Cold-Air Investigation of a Turbine with Transpiration-Cooled Stator Blades. IV - Stage Performance with Wire-Mesh Shell Stator Blading. NASA TM X-2176, 1971.

9. Moffitt, Thomas P.; Prust, Herman W., Jr.; Szanca, Edward M.; and Schum, Harold J.: Summary of Cold-Air Tests of a Single-Stage Turbine with Various Cooling Techniques. NASA TM X-52968, 1971.

10. Whitney, Warren J.; Szanca, Edward M.; Moffitt, Thomas P.; and Monroe, Daniel E.: Cold-Air Investigation of a Turbine for High-Temperature-Engine Application. I - Turbine Design and Overall Stator Performance. NASA TN D-3751, 1967.

11. Stabe, Roy G.: Design and Two-Dimensional Cascade Test of Turbine Stator Blade with Ratio of Axial Chord to Spacing of 0.5. NASA TM X-1991, 1970.

12. Prust, Herman W., Jr.; and Helon, Ronald M.: Effect of Trailing-Edge Geometry and Thickness on the Performance of Certain Turbine Stator Blading. NASA TN D-6637, 1972.

NASA-Langley, 1973 —— 28 E-7106

"The aeronautical and space activities of the United States shall be conducted so as to contribute . . . to the expansion of human knowledge of phenomena in the atmosphere and space. The Administration shall provide for the widest practicable and appropriate dissemination of information concerning its activities and the results thereof."

—NATIONAL AERONAUTICS AND SPACE ACT OF 1958

NASA SCIENTIFIC AND TECHNICAL PUBLICATIONS

TECHNICAL REPORTS: Scientific and technical information considered important, complete, and a lasting contribution to existing knowledge.

TECHNICAL NOTES: Information less broad in scope but nevertheless of importance as a contribution to existing knowledge.

TECHNICAL MEMORANDUMS: Information receiving limited distribution because of preliminary data, security classification, or other reasons. Also includes conference proceedings with either limited or unlimited distribution.

CONTRACTOR REPORTS: Scientific and technical information generated under a NASA contract or grant and considered an important contribution to existing knowledge.

TECHNICAL TRANSLATIONS: Information published in a foreign language considered to merit NASA distribution in English.

SPECIAL PUBLICATIONS: Information derived from or of value to NASA activities. Publications include final reports of major projects, monographs, data compilations, handbooks, sourcebooks, and special bibliographies.

TECHNOLOGY UTILIZATION PUBLICATIONS: Information on technology used by NASA that may be of particular interest in commercial and other non-aerospace applications. Publications include Tech Briefs, Technology Utilization Reports and Technology Surveys.

Details on the availability of these publications may be obtained from:

SCIENTIFIC AND TECHNICAL INFORMATION OFFICE

NATIONAL AERONAUTICS AND SPACE ADMINISTRATION

Washington, D.C. 20546